# *Radio Galaxies and Blazars*



## Introduction, I

The powerful radio galaxy Cygnus A at $z = 0.057$ ($d = 230$ Mpc).

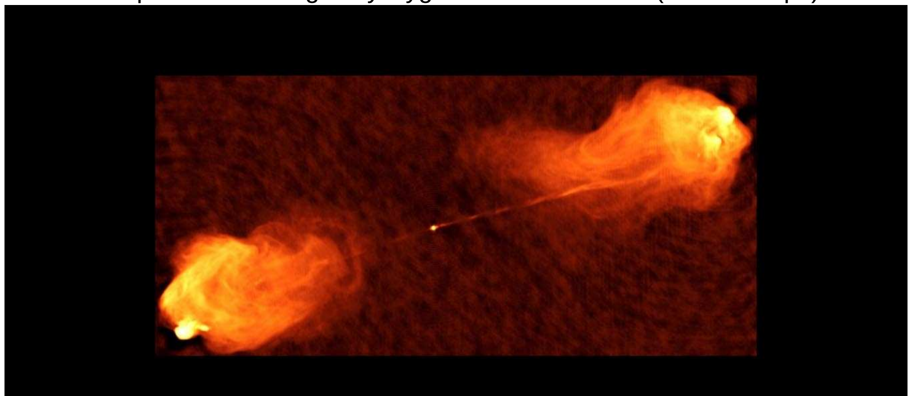

Radio (VLA: 6 cm); Credit: NRAO/AUI

Size: $\sim$ 2.2 arcmin $\sim$ 600000 ly, about eight times the size of the milky way!

Radio morphology: Core – Jets – Hotspots – Lobes





## Introduction, II

The powerful radio galaxy Cygnus A at $z = 0.057$ ($d = 230$ Mpc).

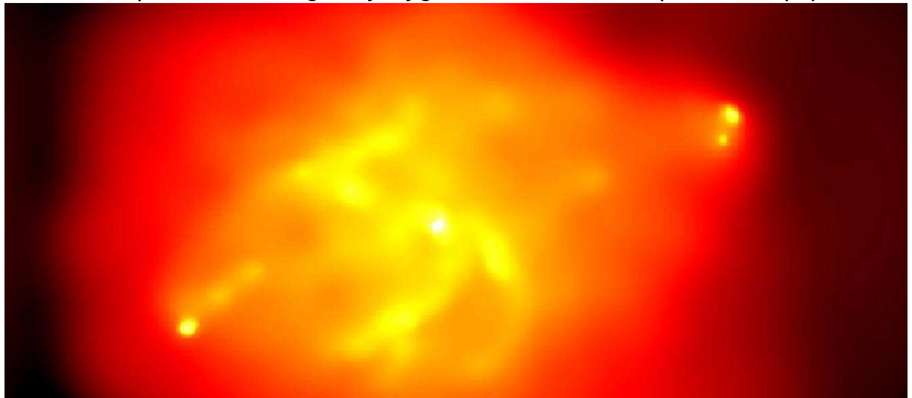

X-Ray (*Chandra*: 0.2 keV – 8 keV); Credit: NASA/UMD/A.Wilson et al.

Size: $\sim$ 2.2 arcmin $\sim$ 600000 ly, about eight times the size of the milky way!

Radio morphology: Core – Jets – Hotspots – Lobes

X-Ray morphology: Nucleus – Cavity – Hotspots



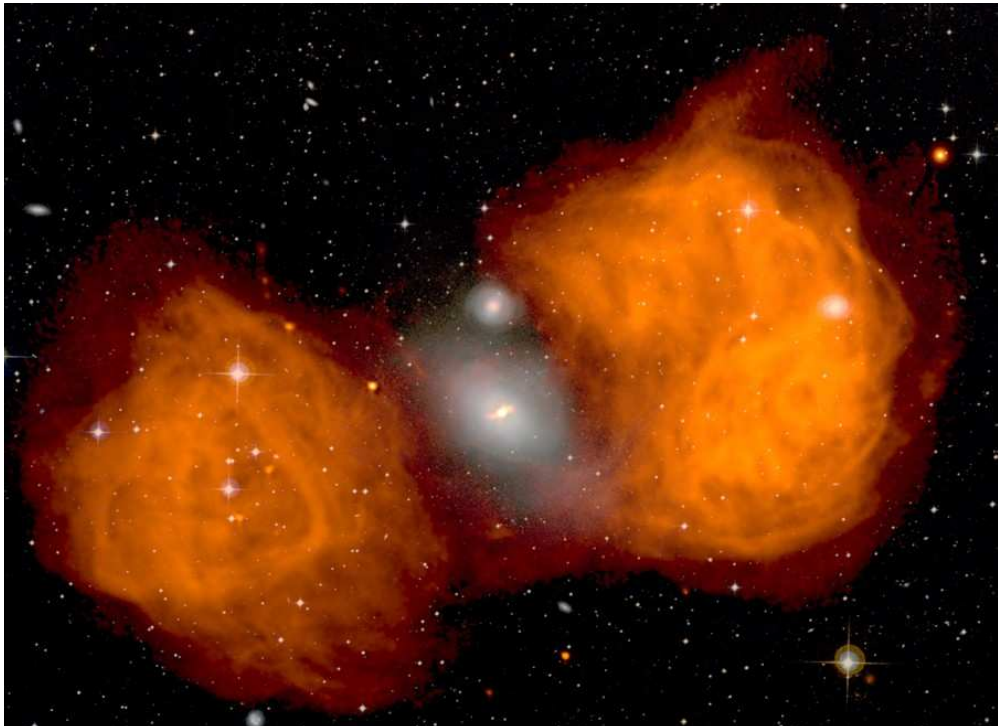

Fornax A: Radio (VLA) overlaid on optical (STScI/POSS-II); Credit: NRAO/AUI and J. M. Uson

## Classification, I

Classification based on morphology and radio spectrum:

1. Powerful double-lobed radio galaxies with hotspots and a steep radio spectrum falling toward higher frequencies (Fanaroff-Riley class II, FR II)
2. Weaker steep-spectrum, double-lobed radio galaxies without leading hotspots (FR I types)
3. Core-dominated flat-spectrum sources (Blazars: quasars and BL Lac objects)
4. Compact steep-spectrum sources (CSS sources) and gigahertz-peaked spectrum sources (GPS sources); no large-scale radio structure; morphological classification term: compact symmetric objects (CSOs) or compact doubles

Observing technique and frequency strongly affects sample composition (e.g., low-frequency flux-density limited surveys tend to select steep-spectrum sources. Flat-spectrum sources are classical targets for Very-Long-Baseline Interferometry (VLBI) observations, which are sensitive to compact emission.



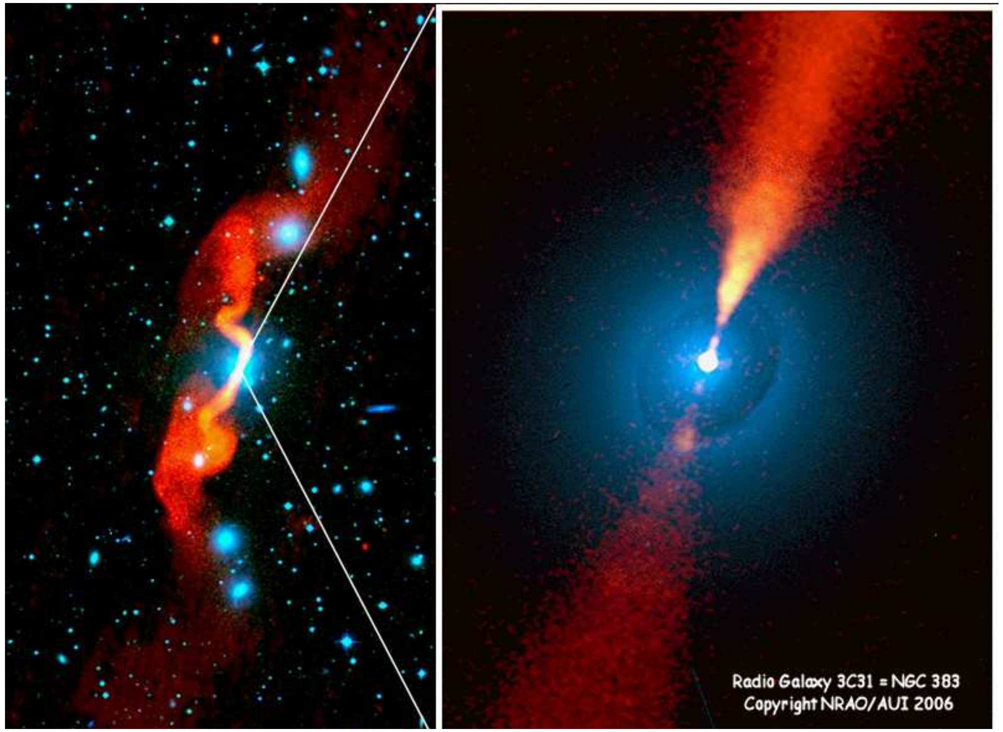


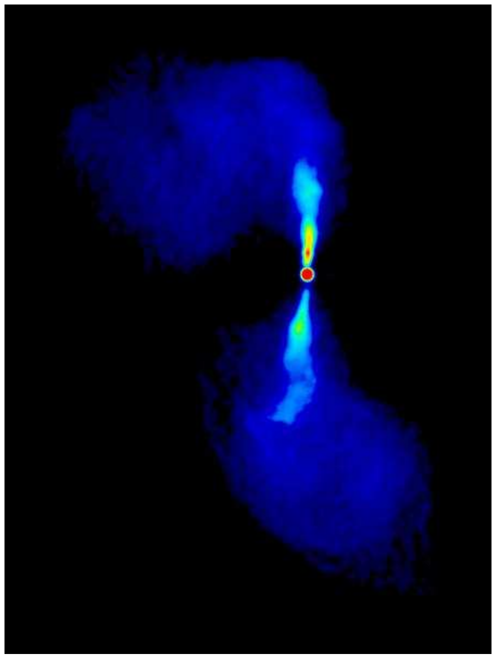

Fanaroff-Riley Type 1: asymmetric jets with wide opening angle ending in plumes

M84 (3C272.1) (Laing & Bridle, 1987):
VLA 4885 MHz, 134″ × 170″; see also
www.jb.man.ac.uk/atlas/other/3C272P1.html

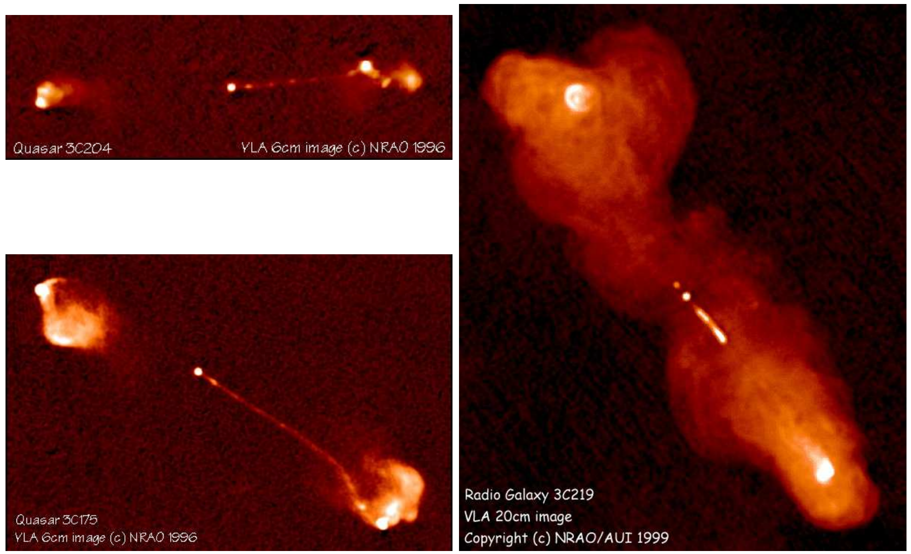


A. Bridle, www.cv.nrao.edu/~abridle/images.htm

Fanaroff-Riley Type 2: powerful lobe dominated doubles; jets often one-sided

Radio Interferometry: Longer baselines and higher frequencies yield higher resolution

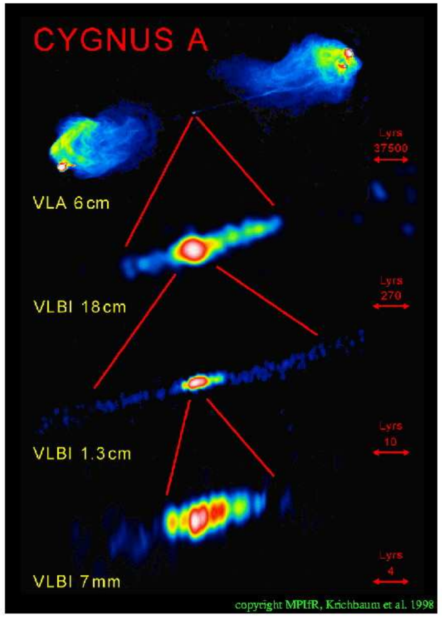


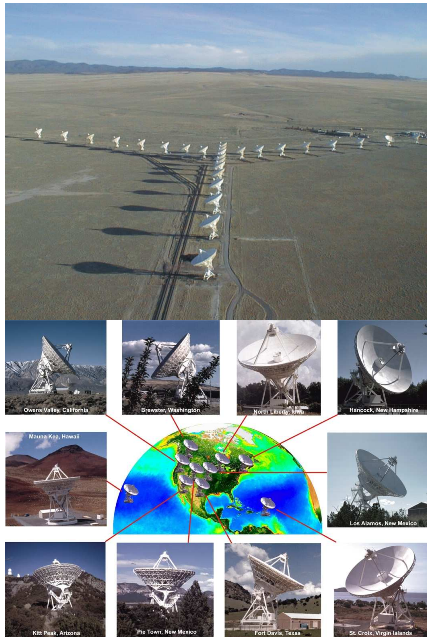

Image courtesy of MPIfR, NRAO/AUI and Earth image courtesy of the SeaWiFS Project NASA/GSFC and ORBIMAGE



## Flat-Spectrum Radio Sources: Blazars

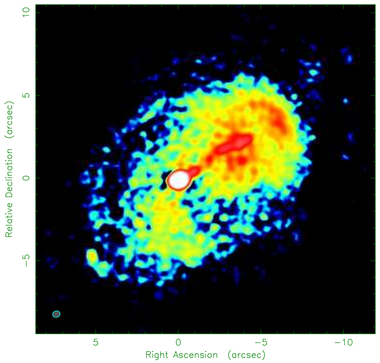


Image courtesy: U. Bach, MPIfR
0716+714, BL Lac object at redshift $z = 0.3$ (Nilsson et al., 2008)
Highly variable, core dominated object
"Fried-egg" morphology – really the end-on view of a radio lobe?

Almost all the flux density is concentrated within a few milliarcseconds-size compact jet!

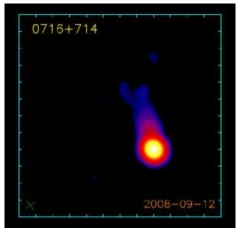


Image Courtesy: MOJAVE

"Roughly equal numbers of steep-spectrum extended double-lobed sources and flat-spectrum objects that are unresolved on arcsec scales." (Zensus, 1997)





## Synchrotron Radiation

Jets are observed to have strong polarization and power law radio spectrum. These are characteristics of synchrotron radiation.

Synchrotron-Radiation (=Magnetobremsstrahlung): Radiation emitted by relativistic electrons in a magnetic field.

*Outline for the following discussion of synchrotron-radiation theory:* Shortened, qualitative description (see Rybicki & Lightman, "Radiative Processes in Astrophysics", Wiley, New York, Chapter 3,6,7 for details):

1. Motion of electrons in magnetic fields
2. Look at emission of one single electron
3. Consider electron distribution and opacity effects to obtain the final spectrum.





## Relativistic Motion

Moving electron in magnetic field ($\boldsymbol{E} = 0$): Lorentz-Force (cgs formulation)

$$\frac{d\boldsymbol{p}}{dt} = \frac{e}{c}\boldsymbol{v} \times \boldsymbol{B} \quad \text{where} \quad \boldsymbol{p} = \frac{m_e \boldsymbol{v}}{\sqrt{1-\beta^2}} = \gamma m_e \boldsymbol{v} \tag{5.1}$$

where $\beta = v/c$.

i.e.:

$$\frac{d\boldsymbol{v}}{dt} = \frac{e}{c\gamma m_e}\boldsymbol{v} \times \boldsymbol{B} \quad . \tag{5.2}$$

Since $\boldsymbol{v} \times \boldsymbol{B}$ is always perpendicular to $\boldsymbol{v}$ and $\boldsymbol{B}$, the component of $\boldsymbol{v}$ along the B-field does not change. Constant acceleration perpendicular to this (circular component) leads to helical motion with the frequency

$$\omega_B = \frac{eB}{\gamma m_e c} = \frac{\omega_L}{\gamma} \tag{5.3}$$

where $\omega_L = 2\pi\nu_L$: Larmor frequency (also Cyclotron frequency, gyrofrequency).

## Numerical values

Numerically, Larmor frequency is

$$\nu_\mathrm{L} = 2.8 B_{1\,\mathrm{G}}\,\mathrm{MHz} \tag{5.4}$$

The radius of the orbit (Larmor radius) is

$$R = \frac{\gamma v_\perp}{\omega_\mathrm{L}} \approx 2\,\mathrm{AU} \cdot \frac{E}{1\,\mathrm{GeV}} \cdot \left(\frac{B}{10^{-6}\,\mathrm{G}}\right)^{-1} \tag{5.5}$$

i.e., small on cosmical scales

$\Longrightarrow$ MHD gets possible (compare SNR discussion).





## Radiated Energy, I

In reality, we will have a large number of electrons with a distribution of velocity vectors and pitch angles with respect to the magnetic field lines. Total energy radiated: Integration over all electrons.

Assumption of isotropic velocity distribution, very fast electrons ( $\beta \longrightarrow 1$), and a messy derivation (see Rybicki & Lightman) yields for the average emitted power:

$$\langle P_\mathrm{em}\rangle = \frac{4}{3}\beta^2\gamma^2 c\sigma_\mathrm{T} U_\mathrm{B} \tag{5.6}$$

with $U_\mathrm{B} = B^2/8\pi$, the magnetic field density, and $\sigma_\mathrm{T} = \frac{8\pi e^2}{3m_\mathrm{e}^2c^4}$, the Thomson cross section.

*Note:* Since $E = \gamma m_\mathrm{e} c^2 \Longrightarrow P \propto E^2 U_\mathrm{B}$.

*Note:* $P_\mathrm{em} \propto \sigma_\mathrm{T} \propto m_\mathrm{e}^{-2} \Longrightarrow$ Synchrotron radiation from charged particles with larger mass (protons,...) is negligible.

*Note:* Life-time of particles of energy $E$ is

$$t_{1/2} \sim \frac{E}{P} \propto \frac{1}{B^2 E} = 5\,\mathrm{s}\left(\frac{B}{1\,\mathrm{T}}\right)^{-2}\gamma^{-1} = 1.6\times 10^7\,\mathrm{years}\left(\frac{B}{10^{-7}\,\mathrm{T}}\right)^{-2}\gamma^{-1} \tag{5.7}$$





## Radiated Energy, II

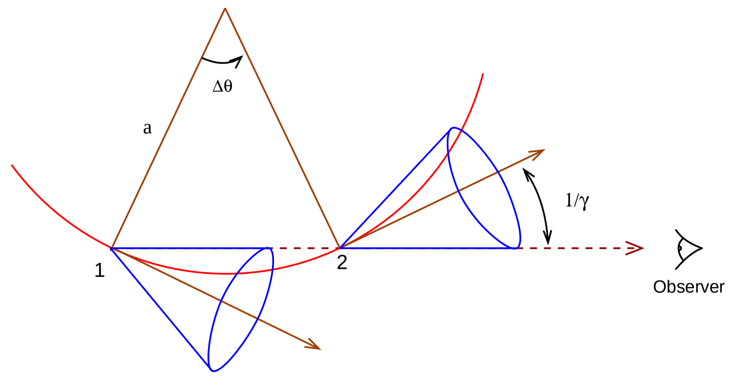


(Rybicki & Lightman, 1979, after Fig. 6.2)

Electron frame of rest: beam passes observer during time

$$\Delta t = \frac{\Delta\theta}{\omega_\mathrm{B}} = \frac{m_\mathrm{e} c\gamma}{eB}\frac{2}{\gamma} = \frac{2}{\omega_\mathrm{L}} \tag{5.8}$$





## Radiated Energy, III

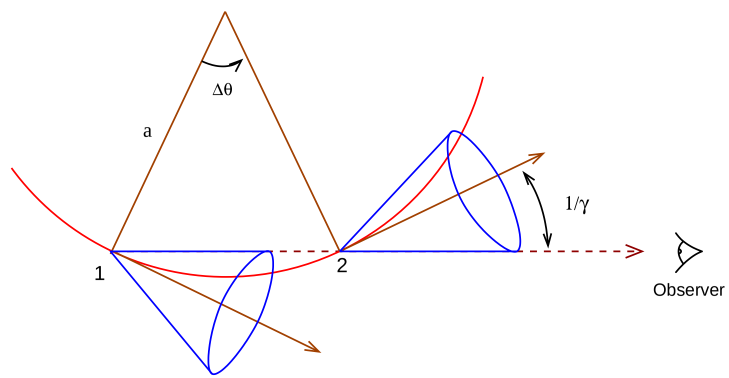


(Rybicki & Lightman, 1979, after Fig. 6.2)

Observer frame: Doppler! (electron is closer at end of beam)

$\Longrightarrow$ observed pulse duration:

$$\tau = \left(1 - \frac{v}{c}\right)\Delta t = (1-\beta)\Delta t \tag{5.9}$$

## Radiated Energy, IV

For $\gamma \gg 1$, i.e., $\beta = v/c \sim 1$

$$\frac{1}{\gamma^2} = 1 - \frac{v^2}{c^2} = (1+\beta)(1-\beta) \approx 2(1-\beta) \tag{5.10}$$

such that

$$\tau = (1-\beta)\Delta t = \frac{1}{2}\left(1 - \frac{v^2}{c^2}\right)\Delta t = \frac{1}{\gamma^2 \omega_\mathrm{L}} \tag{5.11}$$

Thus the characteristic frequency of the radiation is given by

$$\omega_\mathrm{c} = \gamma^2 \omega_\mathrm{L} = \frac{eB}{m_\mathrm{e} c}\left(\frac{E}{m_\mathrm{e}c^2}\right)^2 \tag{5.12}$$

The short gyration pulses produce a wide spectrum (Heisenberg: $\Delta\omega\Delta t > 1$) with the highest frequency in the regime of $\nu_\mathrm{c} = \omega_\mathrm{c}/2\pi$.





## Nonthermal Synchrotron Radiation, I

For an electron distribution, $n(\gamma)$, the emitted spectrum is found by properly weighting contributions of electrons with different energies:

$$P_\nu = \int_1^\infty P_\nu(\gamma) n(\gamma) d\gamma \tag{5.13}$$

Most important case: nonthermal synchrotron radiation, where electrons have a power-law distribution

$$n(\gamma) d\gamma = n_0 \gamma^{-p} d\gamma \quad . \tag{5.14}$$

We have seen that the spectral energy distribution $P_\nu$ of an electron with total energy $E = \gamma m_\mathrm{e} c^2$ can be written as

$$P_\nu(\gamma) = \frac{4}{3}\beta^2\gamma^2 c\sigma_\mathrm{T} U_\mathrm{B} \phi_\nu(\gamma) \tag{5.15}$$

where the spectral shape is described by a function $\phi_\nu(\gamma)$ with

$$\int \phi_\nu(\gamma)\, \mathrm{d}\gamma = 1 \quad . \tag{5.16}$$





## Nonthermal Synchrotron Radiation, II

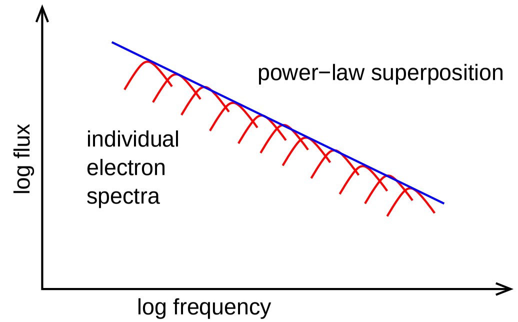


after (Shu, 1991, Fig. 18.4)

Assume that photons are only emitted at frequency $\gamma^2\nu_\mathrm{L}$ (good approximation since the spectrum has strong peak there), i.e.,

$$\phi_\nu(\gamma) \sim \delta(\nu - \gamma^2\nu_\mathrm{L}) \tag{5.17}$$

Therefore the emitted power (=spectrum) is

$$P_\nu = \int_1^\infty \langle P_\nu(\gamma)\rangle\, n(\gamma)\, \mathrm{d}\gamma \tag{5.18}$$





## Nonthermal Synchrotron Radiation, III

Therefore

$$P_\nu = \int_1^\infty \frac{4}{3}\beta^2\gamma^2 c\sigma_\mathrm{T} U_\mathrm{B} \delta(\nu - \gamma^2\nu_\mathrm{L}) n_0 \gamma^{-p}\, \mathrm{d}\gamma \tag{5.19}$$

since $\gamma \gg 1$: $\beta \approx 1$

$$= A \int_1^\infty \gamma^{2-p}\delta(\nu - \gamma^2\nu_\mathrm{L})\, \mathrm{d}\gamma \tag{5.20}$$

substituting $\nu' = \gamma^2\nu_\mathrm{L}$, i.e., $\mathrm{d}\nu' = \nu_\mathrm{L} 2\gamma\, \mathrm{d}\gamma$

$$= B \int_{\nu_\mathrm{L}}^\infty \gamma^{1-p}\delta(\nu - \nu')\, \mathrm{d}\nu' \tag{5.21}$$

since $\gamma = (\nu'/\nu_\mathrm{L})^{1/2}$, we find

$$P_\nu = \frac{2}{3} c\sigma_\mathrm{T} n_0 \frac{U_\mathrm{B}}{\nu_\mathrm{L}} \left(\frac{\nu}{\nu_\mathrm{L}}\right)^{-\frac{p-1}{2}} \tag{5.22}$$

The spectrum of an electron power-law distribution is a power-law!

## Summary

What we have done so far:

1. Motion of the electron
2. Radiation characteristic from relativistic motion
3. Doppler-effect
4. Integration over electron distribution

It is possible to do the same analytically without any approximations. This is too complicated to be done here. See the references for details.





## Synchrotron Self-Absorption

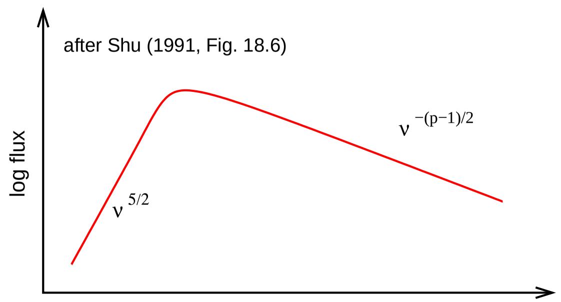


At low $\nu$: synchrotron emitting electrons can absorb synchrotron photons:
synchrotron self-absorption.

For a power law electron distribution $\propto E^{-p}$, total spectral shape is:

For low frequencies: $P_\nu \propto B^{-1/2}\nu^{5/2}$ (independent of $p$!)
For large frequencies: $P_\nu \propto \nu^{-(p-1)/2}$

One often uses the terms optically thick/thin to describe the absorbed/unabsorbed part of a synchrotron spectrum. The turnover describes the $\tau = 1$ surface, e.g., of a jet. In general: $\tau \propto R$ ($R$: size of the emitting region). More compact regions are optically thick, more extended regions are optically thin.





## Example: Cygnus A

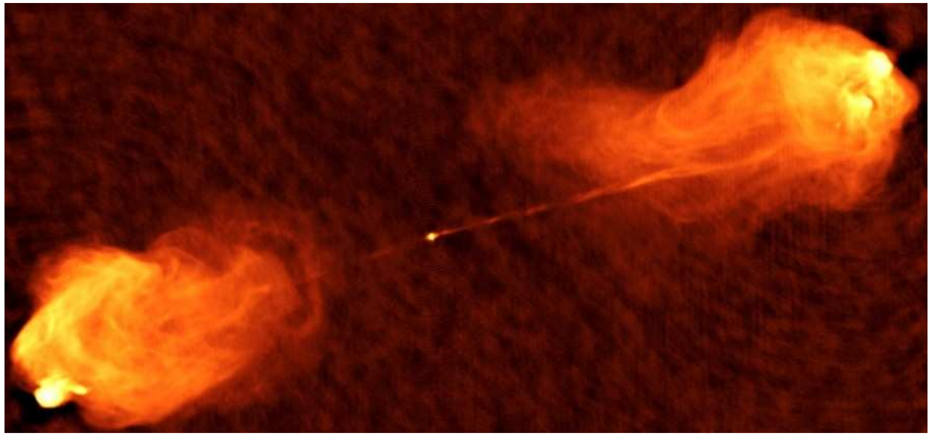

Morphology of radio galaxies suggests that matter is transported along two channels (jets) from the center of the system (core) to the outer regions (here: lobes): What is the speed?





## Apparent Superluminal Motion, I

VLBI resolution 1 mas

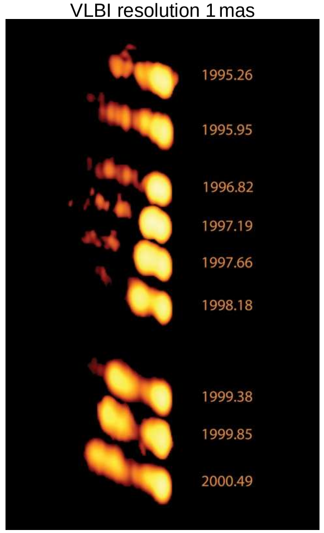


Kadler et al. (2008)

3C 111: Apparent speed of jet: $\sim 5c$

Superluminal motion: The apparent velocities of jet features ("blobs") measured in many AGN jets are $v > c$.

First discovered in 1971 in 3C279
(Cohen et al., 1971; Whitney et al., 1971).

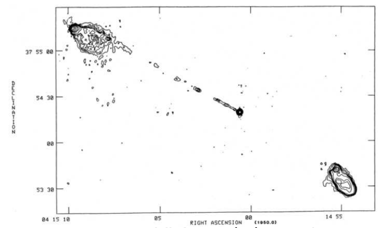

VLA resolution $\sim$ 1 arcsec

Superluminal Motion Demo:

www.physics.purdue.edu/MOJAVE/superluminal.swf

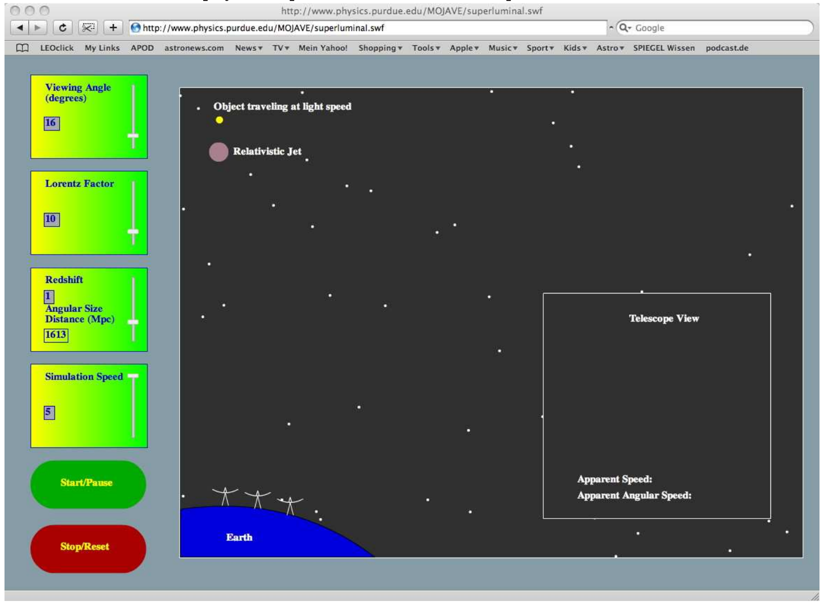


$t_1 = 0$: Blob is ejected from core and emits first photon.

Superluminal Motion Demo:

www.physics.purdue.edu/MOJAVE/superluminal.swf

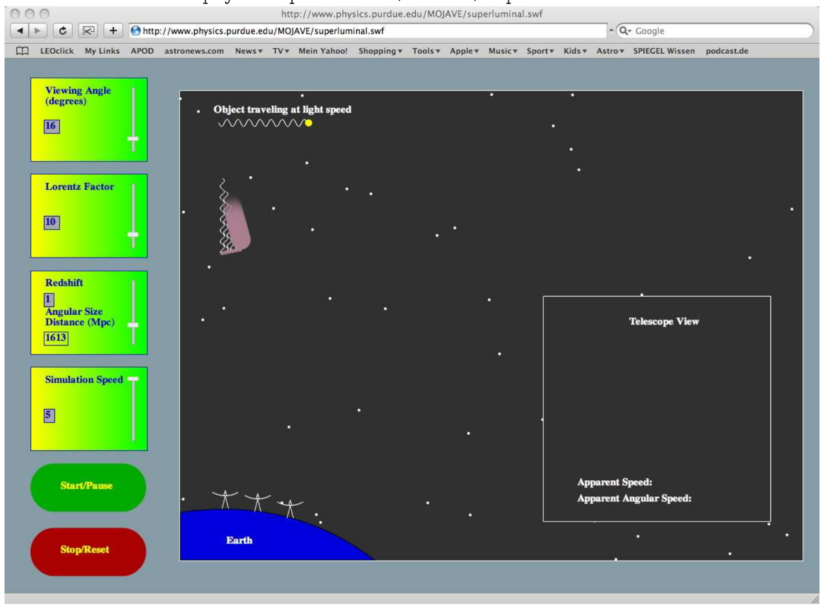


$t_2$: First photons and blob travel towards earth.

Superluminal Motion Demo:

www.physics.purdue.edu/MOJAVE/superluminal.swf

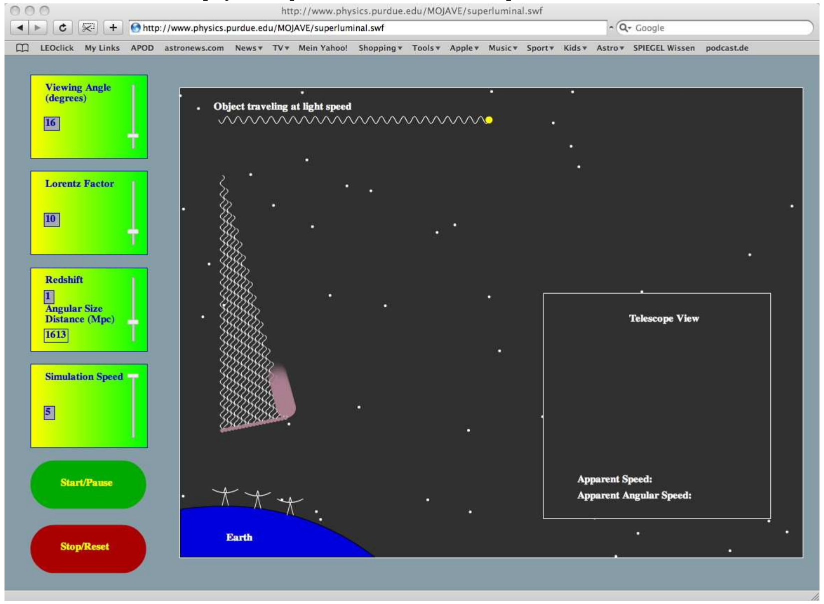


$t_3$: Blob almost keeps the pace of the photons.

Superluminal Motion Demo:

www.physics.purdue.edu/MOJAVE/superluminal.swf

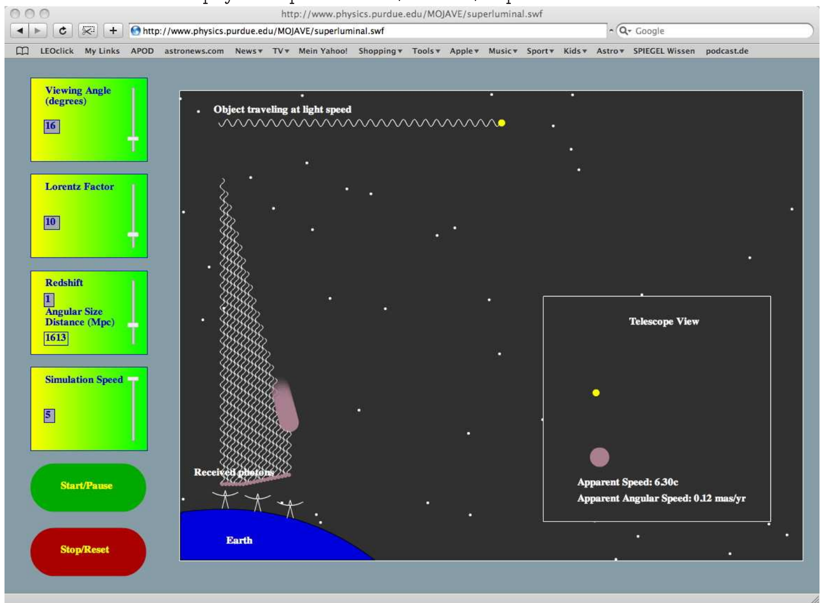


$t_4$: First photons arrive at telescope. Observer starts to take the time.

Superluminal Motion Demo:

`www.physics.purdue.edu/MOJAVE/superluminal.swf`

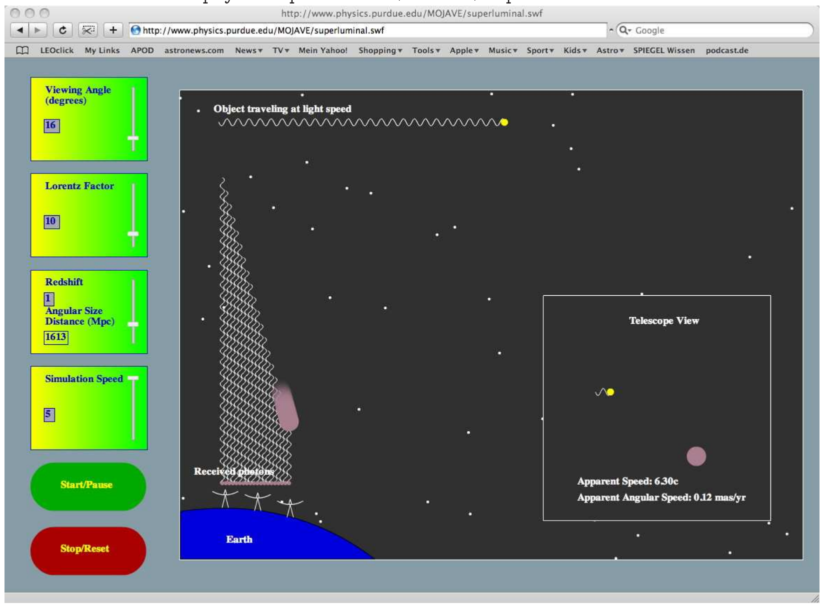


$t_5$: The last photons have a much smaller way to travel and come in quickly.
Observer measures superluminal motion on the sky!



## Apparent Superluminal Motion, VII

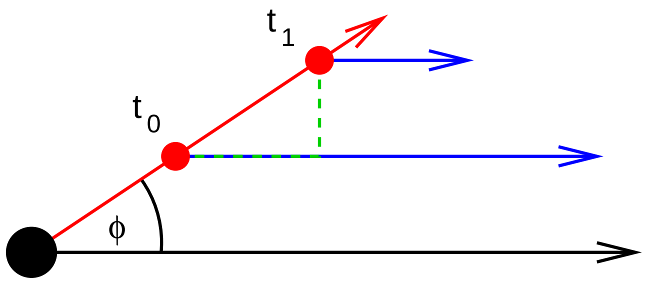


Consider blob moving towards us with speed $v$ and angle $\phi$ with respect to line of sight, emitting light signals at $t_0$ and $t_1 = t_0 + \Delta t_e$

Light travel time: Observer sees signals separated by

$$\Delta t_o = \Delta t_e - \Delta t_e \frac{v}{c} \cos\phi = \left(1 - \frac{v}{c}\cos\phi\right) \Delta t_e \qquad (5.23)$$

Observed distance traveled in plane of sky:

$$\Delta \ell_\perp = v \Delta t_e \sin\phi \qquad (5.24)$$





## Apparent Superluminal Motion, VIII

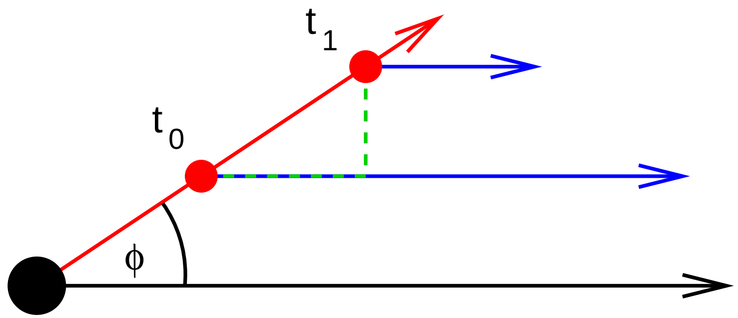


Apparent velocity deduced from observations:

$$v_{\text{app}} = \frac{\Delta \ell_\perp}{\Delta t_o} = \frac{v \Delta t_e \sin\phi}{\left(1 - \frac{v}{c}\cos\phi\right) \Delta t_e} = \frac{v \sin\phi}{\left(1 - \frac{v}{c}\cos\phi\right)} \qquad (5.25)$$

$\Longrightarrow$ For $v/c$ large and $\phi$ small: $v_{\text{app}} > c$





## Apparent Superluminal Motion, IX

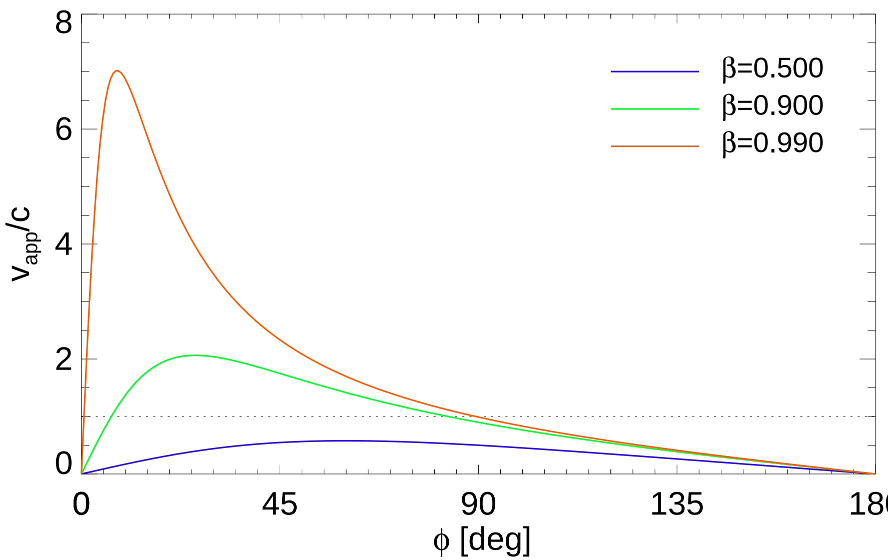

## Relativistic Boosting, I

If jet plasma is moving at relativistic speeds, we have to consider also other relativistic effects.

Remember that

$$\nu = \frac{1}{\Delta t_{\mathrm{A}}} = \frac{\nu'}{\gamma\left(1-\frac{v}{c}\cos\theta\right)} \tag{5.26}$$

and

$$\gamma = \frac{1}{\sqrt{1-\frac{v^2}{c^2}}} \quad . \tag{5.27}$$

This defines the relativistic Doppler factor

$$\mathcal{D} = \frac{1}{\gamma\left(1-\frac{v}{c}\cos\theta\right)} = \frac{\sqrt{1-\beta^2}}{1-\beta\cos\theta} \tag{5.28}$$

(the difference to the classical Doppler factor is only the $\gamma$ factor).

The Doppler factor is a strong function of the aspect angle and can become very large for $v \longrightarrow c$.





## Relativistic Boosting, II

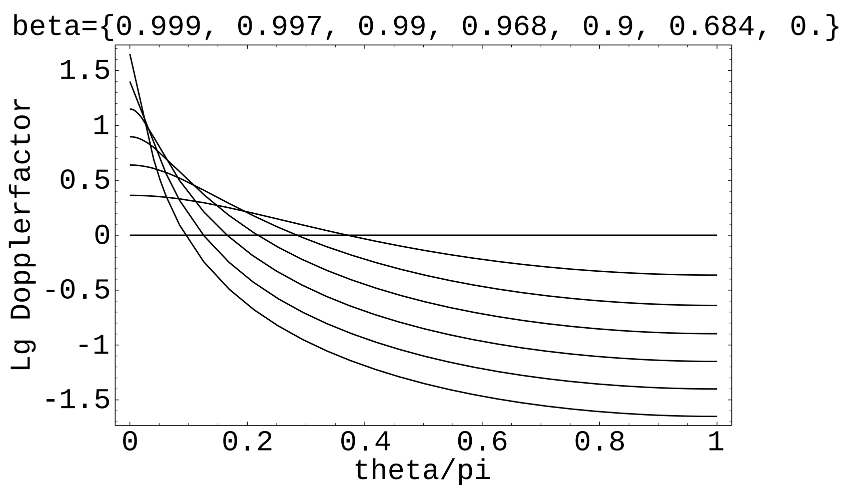


Within $\sim 1-2$ deg, the Doppler factor can approach values of 100 or higher.





## Relativistic Boosting, III

One can show (i.e., Rybicki & Lightman, chap. 4.9) that $S_\nu/\nu^3$ is invariant under Lorentz transformation, where $S_\nu$ is the flux density.

Therefore, observed intensity of a moving blob:

$$\frac{I(\nu_{\mathrm{obs}})}{\nu_{\mathrm{obs}}^3} = \frac{I(\nu_{\mathrm{em}})}{\nu_{\mathrm{em}}^3} \tag{5.29}$$

and

$$I(\nu_{\mathrm{obs}}) = \nu_{\mathrm{obs}}^3 \frac{I(\nu_{\mathrm{em}})}{\nu_{\mathrm{em}}^3} = \mathcal{D}^3 I(\nu_{\mathrm{em}}) \tag{5.30}$$

Specifically, for a blob with a power law spectrum ($I(\nu) = A\nu^\alpha$):

$$I(\nu_{\mathrm{obs}}) = \mathcal{D}^3 A\nu_{\mathrm{em}}^\alpha = \mathcal{D}^3 A\mathcal{D}^{-\alpha}\nu_{\mathrm{obs}}^\alpha \tag{5.31}$$

$$I(\nu_{\mathrm{obs}}) = \mathcal{D}^{3-\alpha} I(\nu_{\mathrm{em}}) \quad . \tag{5.32}$$

Even for relatively modest relativistic velocities of $0.97c$ ($\gamma \simeq 4$), for example, the flux in the forward direction can be boosted by a factor 1000, while it is reduced by a factor 1000 in the backward direction!





## Jet One-Sidedness, I

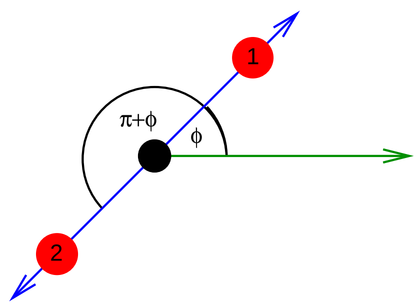


Now take a source emitting blobs symmetrically in two directions.

From Eq. (5.31) the ratio of fluxes from the blobs is

$$\frac{F_1}{F_2} = \left(\frac{1+\beta\cos\phi}{1-\beta\cos\phi}\right)^{3-\alpha} \tag{5.33}$$

Even for mildly relativistic speeds and large angles, features on the approaching side are always significantly brighter than on the receding side.

Jet can be expressed as a series of blobs. But the number of blobs observed scales as the Doppler factor, such that for jets:

$$\frac{F_1}{F_2} = \left(\frac{1+\beta\cos\phi}{1-\beta\cos\phi}\right)^{2-\alpha} \tag{5.34}$$

One sidedness of jets is a relativistic effect!

## Jet One-Sidedness, II

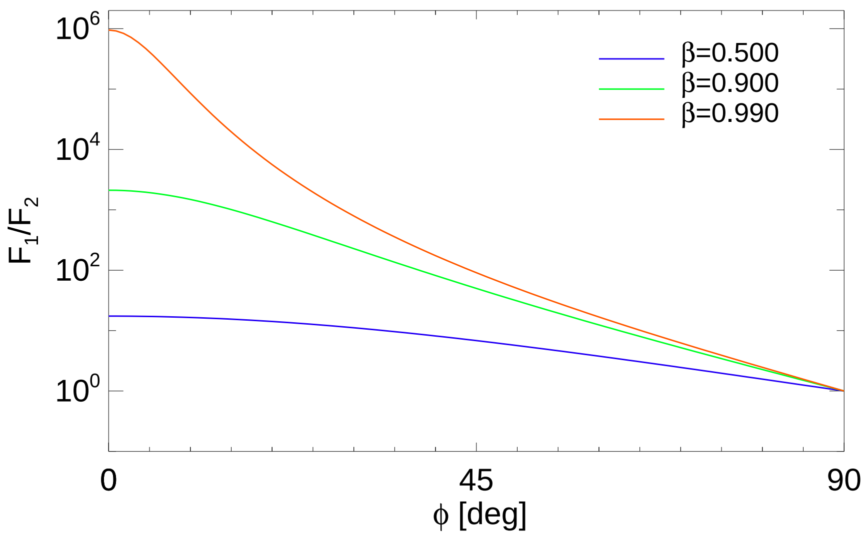




Survey and monitoring of extragalactic jets on parsec scales with the VLBA since 1995

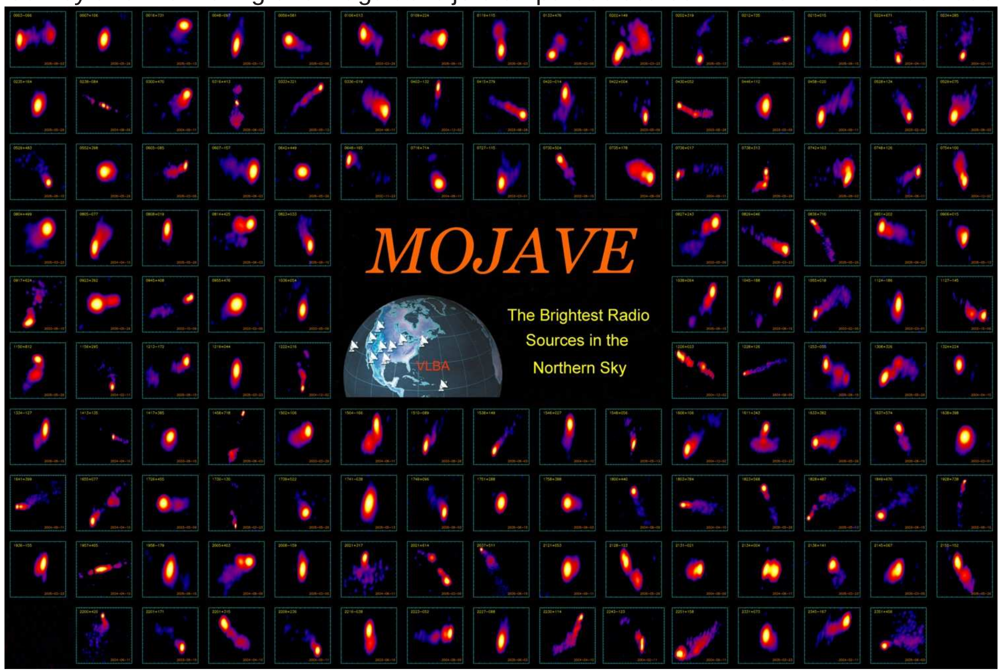


http://www.physics.purdue.edu/astro/MOJAVE/



## Kinematics of Relativistic Jets

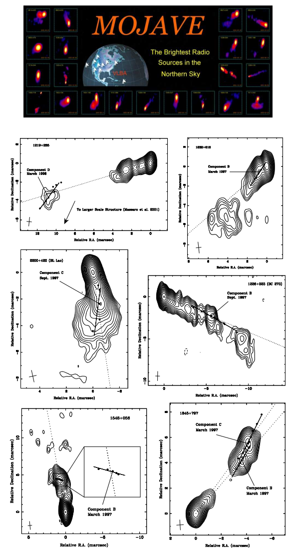


- **MOJAVE**: **M**onitoring **Of J**ets in **A**ctive galactic nuclei with **V**LBA **E**xperiments; Lister et al. (submitted to ApJ)
- Wavelength $\lambda = 2$ cm (15 GHz)
- Statistically complete sub-sample: All flat-spectrum ($\alpha < 0.5$) sources whose compact flux density ever reached 1.5 Jy (2 Jy for southern sources)
- Extended sample includes all known gamma-ray blazars (newly detected *Fermi* sources to be added as of January 2009)
- Results, images and movies at `http://www.physics.purdue.edu/astro/MOJAVE/`
- Observing strategy optimized for each individual source (fast sources are observed every month, slower sources less frequently)





## Kinematics of Relativistic Jets

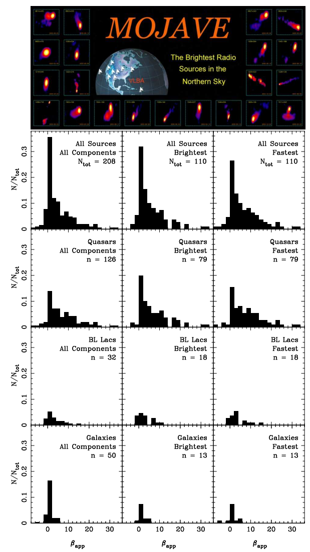


**MOJAVE Results:**

- Distribution of observed velocities typically between 0 and 15$c$: Quasars: tail up to $\beta_{\rm app} \sim 34$; BL Lacs and galaxies: mainly $\beta \lesssim 6$
- In the same jet, different components tend to have similar speeds; but there are exceptions
- In many sources, bent trajectories are seen, which do not back-extrapolate to the core: no cannon-balls!
- Observed pattern speed does not necessarily agree with beam speed
- Most of the flux-density originates in still unresolved regions smaller than 0.05 mas
- High-energy (gamma-ray) emitters have faster and more compact jets

(Kellermann et al., 2004; Kovalev et al., 2005; Cohen et al., 2007)

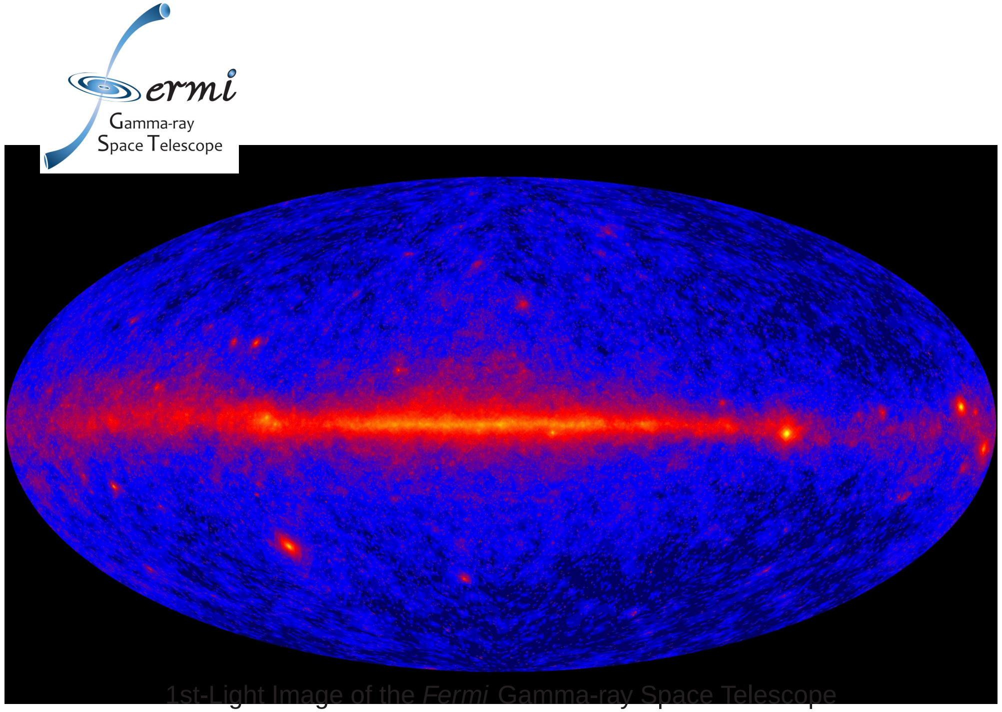


1st-Light Image of the *Fermi* Gamma-ray Space Telescope
(one week of data in August 2008)

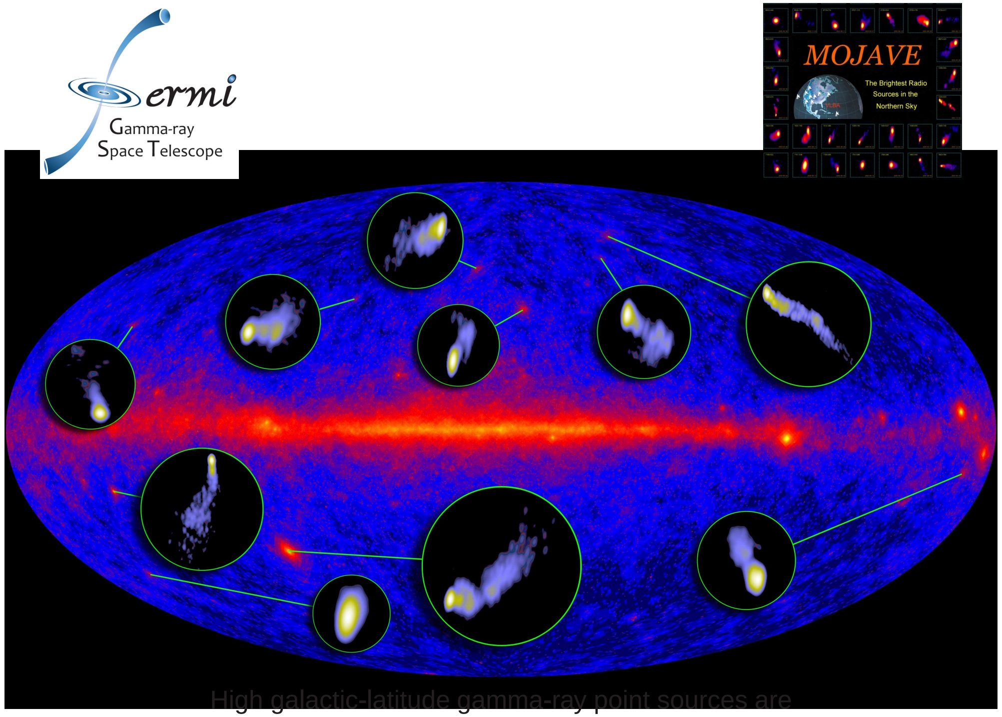


High galactic-latitude gamma-ray point sources are
flat-spectrum radio quasars and BL Lac objects




Cohen, M. H., Cannon, W., Purcell, G. H., Shaffer, D. B., Broderick, J. J., Kellermann, K. I., & Jauncey, D. L., 1971, ApJ, 170, 207

Cohen, M. H., Lister, M. L., Homan, D. C., Kadler, M., Kellermann, K. I., Kovalev, Y. Y., & Vermeulen, R. C., 2007, ApJ, 658, 232

Kadler, M., et al., 2008, ApJ, 680, 867

Kellermann, K. I., et al., 2004, ApJ, 609, 539

Kovalev, Y. Y., et al., 2005, AJ, 130, 2473

Laing, R. A., & Bridle, A. H., 1987, MNRAS, 228, 557

Nilsson, K., Pursimo, T., Sillanpää, A., Takalo, L. O., & Lindfors, E., 2008, A&A, 487, L29

Rybicki, G. B., & Lightman, A. P., 1979, Radiative Processes in Astrophysics, (New York: Wiley)

Shu, F. H., 1991, The Physics of Astrophysics, Vol. I. Radiation, (Mill Valley, CA: University Science Books)

Whitney, A. R., et al., 1971, Science, 173, 225

Zensus, J. A., 1997, ARA&A, 35, 607